

## Articles

**Structural Determinants of *Torpedo californica* Acetylcholinesterase Inhibition by the Novel and Orally Active Carbamate Based Anti-Alzheimer Drug Ganstigmine (CHF-2819)<sup>†</sup>**

Cecilia Bartolucci,<sup>‡</sup> Mariacristina Siotto,<sup>‡</sup> Eleonora Ghidini,<sup>§</sup> Gabriele Amari,<sup>§</sup> Pier Tonino Bolzoni,<sup>§</sup> Marco Racchi,<sup>||</sup> Gino Villetti,<sup>§</sup> Maurizio Delcanale,<sup>§</sup> and Doriano Lamba<sup>\*,⊥</sup>

Istituto di Cristallografia, Consiglio Nazionale delle Ricerche, Area della Ricerca di Roma, P.O. Box 10, I-00016 Monterotondo Stazione (Roma), Italy, Chiesi Farmaceutici SpA, Research & Development, Chemistry and Pharmacology Departments, Via Palermo 26/A, I-43100 Parma, Italy, Department of Experimental and Applied Pharmacology, University of Pavia, Via Taramelli 14, I-27100 Pavia, Italy, and Istituto di Cristallografia, Consiglio Nazionale delle Ricerche, Sezione Staccata di Trieste, Area Science Park - Basovizza S.S. 14 Km 163.5, I-34012 Trieste, Italy

Received March 14, 2006

Ganstigmine is an orally active, geneserine derived, carbamate-based acetylcholinesterase inhibitor developed for the treatment of Alzheimer's disease. The crystal structure of the ganstigmine conjugate with *Torpedo californica* acetylcholinesterase (TcAChE) has been determined at 2.40 Å resolution, and a detailed structure-based analysis of the in vitro and ex vivo anti-AChE activity by ganstigmine and by new geneserine derivatives is presented. The carbamoyl moiety is covalently bound to the active-site serine, whereas the leaving group geneseroline is not retained in the catalytic pocket. The nitrogen atom of the carbamoyl moiety of ganstigmine is engaged in a key hydrogen-bonding interaction with the active site histidine (His440). This result offers an explanation for the inactivation of the catalytic triad and may account for the long duration of action of ganstigmine in vivo. The 3D structure also provides a structural framework for the design of compounds with improved binding affinity and pharmacological properties.

**Introduction**

Alzheimer's disease (AD) is a progressive neurodegenerative disorder and one of the most common causes of mental deterioration in the elderly. It is characterized by the development of senile plaques and neurofibrillar tangles, which are associated with neuronal loss.<sup>1</sup>

The past two decades have witnessed a considerable research effort devoted to unraveling the molecular, biochemical, and cellular mechanisms of AD. Several hypotheses have been proposed attempting to explain the pathogenesis of AD, including theories involving amyloid deposition, tau hyperphosphorylation, inflammation, oxidative stress, and metal ion dysregulation. Consequently, new therapeutic approaches that target these aspects of AD pathology and hold promise for disease modification are currently under development.<sup>2</sup>

Although much progress has been made in this area, interventions able to halt or slow disease progression are as yet unproven, and presently, treatment of AD patients continues to be mainly symptomatic, with cholinesterase (ChE) inhibitors as first-line drugs.<sup>3</sup>

The development of ChE inhibitors was based on the well-accepted cholinergic hypothesis, which states that the deficits in learning, memory, and behavior associated with AD are caused, at least in part, by the loss of cortical cholinergic

neurotransmission.<sup>3</sup> This was later supported by clinical trials showing an improvement on cognition and global function in AD patients after treatment with ChE inhibitors, with little impact on the eventual progression of the disease.<sup>4,5</sup> As a result, over the past decade, various ChE inhibitors have been launched on the market, such as the synthetic compounds tacrine (Cognex, originally Pfizer Inc. & Warner-Lambert, currently First Horizon Pharm Corp.), donepezil (Aricept, Pfizer Inc. & Eisai Corp.), and rivastigmine (Exelon, Novartis) or the natural substance galanthamine (Reminyl, Janssen). In October 2003, a *N*-methyl-D-aspartate receptor antagonist, memantine (Namenda, Merz Pharma & Forest Labs.), also has been approved for the treatment of moderate to severe AD.

Recently, a new dimension to the question of specificity with regard to AChE inhibitors emerged as molecular cloning of AChE genes from different species revealed that alternative splicing gives rise to three distinct AChE isoforms: the synaptic, the erythrocytic, and the rare readthrough. The latter was discovered to undergo dramatic up-regulation under some conditions, including acute psychological stress and exposure to AChE inhibitors.<sup>6,7</sup>

Physostigmine (PHY) and geneserine ((GEN), Figure 1) are the two major alkaloids present in Calabar beans. Analogues to PHY, heptylphysostigmine,<sup>8</sup> phenserine,<sup>9</sup> and 8-(*cis*-2,6-dimethylmorpholino)octylcarbamoyl-ereseroline (MF268),<sup>10–12</sup> ChE inhibitors with different pharmacodynamic and pharmacokinetic profiles and different degrees of selectivity upon the two forms of ChE, that is, acetylcholinesterase (AChE) and butyrylcholinesterase (BuChE), were thoroughly studied as potential drugs for AD.<sup>13</sup> A series of new aryl and alkyl GEN analogues have been synthesized and their biological activity described.<sup>14–17</sup> In particular, the pre-clinical profile of the

<sup>†</sup> The atomic coordinates and structure factor amplitudes of the TcAChE–ganstigmine complex have been deposited in the Brookhaven Protein Data Bank under pdb ID code 2BAG.

\* Corresponding author. Tel: +39-040-226881. Fax: +39-040-9221126. E-mail: doriano.lamba@ic.cnr.it; doriano.lamba@elettra.trieste.it.

<sup>‡</sup> Istituto di Cristallografia, Roma.

<sup>§</sup> Chiesi Farmaceutici SpA.

<sup>||</sup> University of Pavia.

<sup>⊥</sup> Istituto di Cristallografia, Trieste.

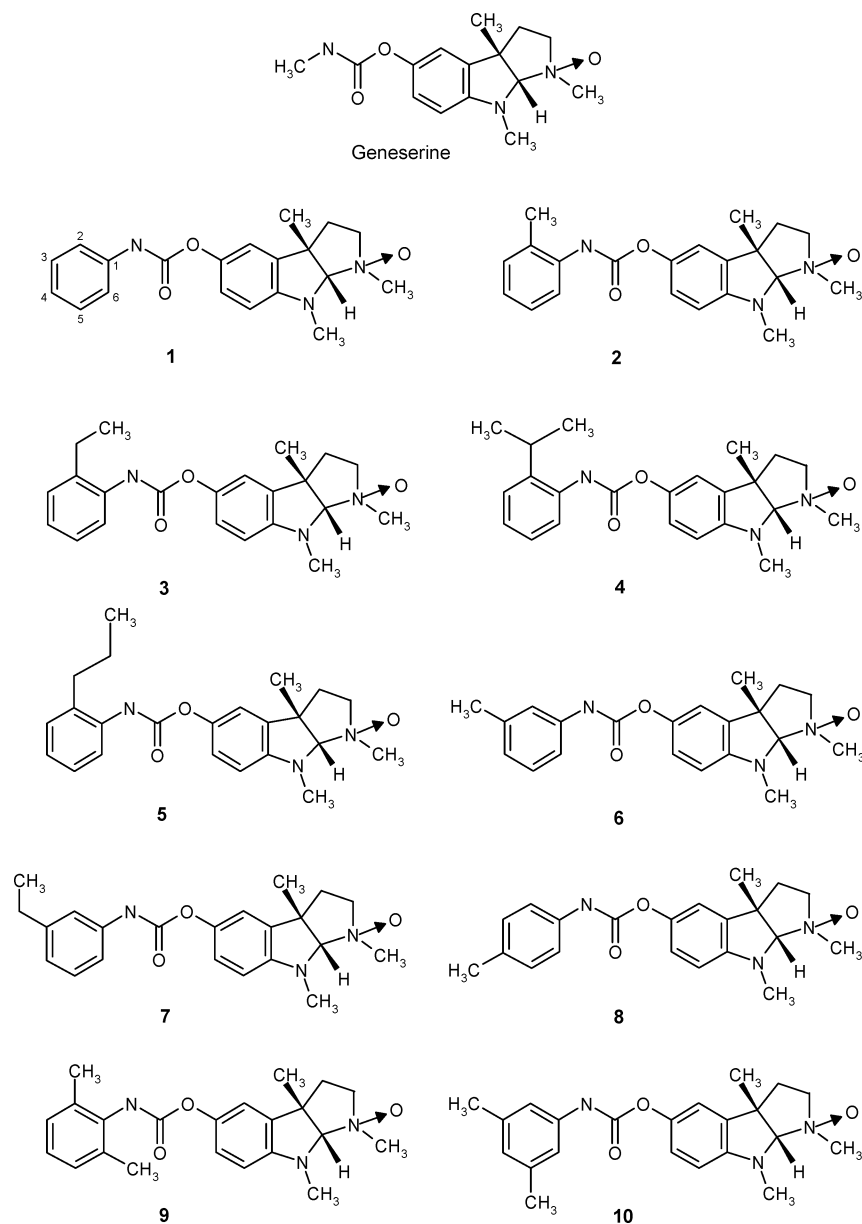


**Figure 1.** Chemical structures of geneserine and new aryl derivatives.

carbamate-based, orally active AChE inhibitor, ganstigmine, (–)-*O*-[(2'-ethylphenyl)carbamoyl]geneseroline hydrochloride (CHF-2819) (**3**) (Figure 1) was evaluated, and this compound showed potential for the treatment of AD.<sup>18–24</sup>

The results of first clinical trials evaluating the safety, tolerability, and pharmacodynamics of ganstigmine in AD patients are now available.<sup>25</sup> Furthermore, intraperitoneal and oral administration of ganstigmine was shown to rescue the neurodegenerative phenotype in AD11 anti-nerve growth factor mice, a transgenic model for AD.<sup>26</sup> Recently, the anti-cholinesterase activity of GEN analogues that can undergo tautomerism between the *N*-oxide and the 1,2-oxazine structures in a pH- and time-dependent manner has been assessed.<sup>27</sup>

An analysis of the X-ray crystal structure of the newly discovered, carbamate-based, orally active inhibitor **3** in complex with *Torpedo californica* (*Tc*) AChE is of particular significance to elucidate its mechanism of inhibition at the molecular level. Furthermore, the knowledge of the crystal structure of the complex offers a starting point for a structure–activity evaluation of a number of synthetic modifications of GEN aimed at improving their anticholinesterase activity, binding character-

istics (duration of action), and ability to differentially inhibit the two subtypes of ChE enzymes.

## Results and Discussion

### Interaction of Ganstigmine with Acetylcholinesterase.

GEN and its derivatives belong to a large class of carbamate-like inhibitors whose mechanism of action is characterized by a fast carbamylation of the esteratic site of the enzyme, followed by a slow regeneration of the active enzyme.

The crystal structure of *Tc*AChE in complex with **3** has been determined at 2.40 Å resolution. It reveals that the (2'-ethylphenyl) carbamic moiety is covalently bound to the O $\gamma$  of Ser200 (Figure 2), whereas the leaving group geneseroline is not retained in the catalytic pocket.

An analogous situation was reported for the *Tc*AChE–MF268 conjugate (pdb accession code: 1OCE),<sup>28</sup> where the carbamoyl moiety, the (*cis*-2,6-dimethylmorpholino) octyl chain, stretches along the active-site gorge, and the leaving group eseroline is not retained either. In both complexes, no substantial conformational changes relative to the native enzyme structures (pdb

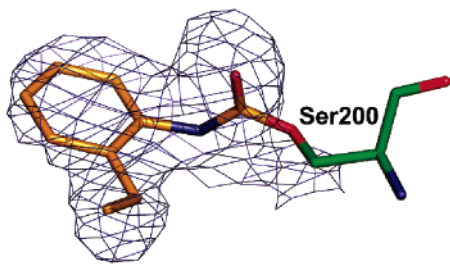
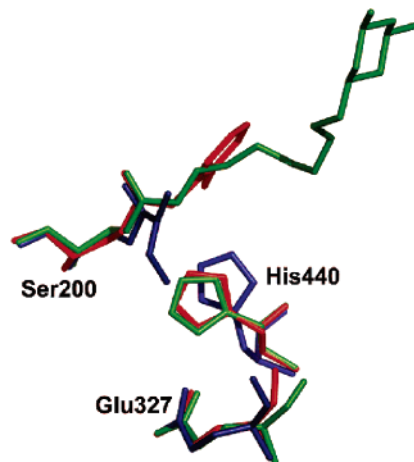


**Figure 2.** Structure of the covalent reaction product of the carbamic moiety of ganstigmine with the catalytic Ser200 of *TcAChE*. View of the refined structure of the 2'-ethylphenyl moiety of ganstigmine in the active site of *TcAChE* superimposed on the initial  $\sigma_a$  weighted ( $|F_o| - |F_c|$ ,  $\phi_c$ ) density map (27.95–2.40 Å all data, map contour level  $2.5\sigma$ ) was computed after initial refinement of the native protein by simulated annealing, followed by maximum likelihood positional and individual isotropic temperature factor restrained refinements.

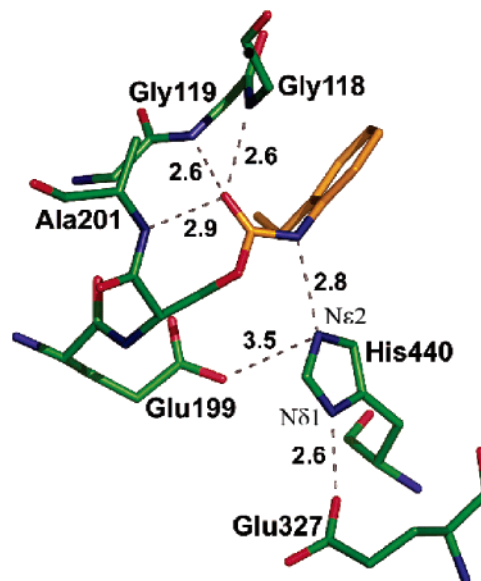
accession codes: 2ACE and 1EA5)<sup>29,30</sup> were observed upon carbamylation. Overall, the present finding supports the hypothesis of the existence of a route, viz. a back door, for the clearance of the bulky geneseroline moiety as proposed for eseroline in the *TcAChE*–MF268 complex.<sup>28</sup> A transient opening of a short channel, through a thin wall of *TcAChE* near the substrate binding site, Trp84, has been hypothesized<sup>31</sup> and has since been the object of controversy,<sup>32–35</sup> but it continues to elude definite experimental proof. Interestingly, the crystal structure of *TcAChE* in complex with a bivalent derivative of galanthamine<sup>36</sup> showed that the native conformation of the Trp279–Ser291 loop can be severely disrupted, suggesting that additional regions of the gorge can undergo substantial movement, making it possible for the bulky leaving groups to escape. Recently, the crystal structures of *TcAChE* complexed with the substrate acetylthiocholine, the product thiocholine, and the nonhydrolyzable substrate 4-oxo-*N,N,N*-trimethylpentanaminium provided structural insight into substrate traffic and inhibition.<sup>37</sup>

**Structural Determinants of Enzyme Inactivation and Comparison with Other Inhibitors.** It is noteworthy that the crystal structure of the *TcAChE*–rivastigmine conjugate (pdb accession code: 1GQR)<sup>38</sup> although revealing, as anticipated, the carbamoyl moiety to be covalently linked to the active-site serine, showed the leaving group, (–)-*S*-3-[1-(dimethylamino)-ethyl]phenol, to be retained in the active-site gorge. A significant movement of the active site His440 away from its normal hydrogen-bonded partner Glu327 was observed, resulting in the disruption of the catalytic triad (Figure 3) and providing a possible explanation for the unusually slow kinetics of reactivation. The occurrence of a mobile and conformationally heterogeneous catalytic histidine in acetylcholinesterase reactions has been demonstrated, and its optimal functional configuration relative to other elements of the catalytic triad has been thoroughly analyzed.<sup>39–45</sup>

An overlay of the MF268 and the ganstigmine conjugate structures shows that as previously observed for the *cis*-2,6-dimethylmorpholinoethyl chain<sup>28</sup> the binding of the 2'-ethylphenyl carbamic moiety (ganstigmine) does not alter the position and orientation of the residues belonging to the catalytic triad (Figure 3). It should be noted that in the *TcAChE*–rivastigmine structure the position of the main chain ( $C^\alpha$ ) carbon atom of His440 moves by 0.64 Å relative to its position in the native enzyme structure.<sup>29,30</sup> However, it is important to observe, that the distances between the N atom of the carbamic moiety (donor) and  $N^{\epsilon 2}$  of His440 (acceptor) are 3.26 Å and 4.34 Å in MF268<sup>28</sup> and rivastigmine<sup>38</sup> *TcAChE* conjugates, respectively, and only 2.83 Å in the present structure. The existence of this



**Figure 3.** Position and orientation of His440 in the active site of *TcAChE*. The structures depicted are those of the *TcAChE*–MF268 (green),<sup>28</sup> *TcAChE*–rivastigmine (blue),<sup>38</sup> and *TcAChE*–ganstigmine (red) conjugates. An overlay of the catalytic triad in the three structures is presented.

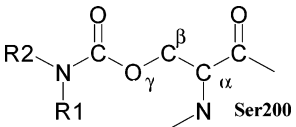


**Figure 4.** Binding mode of the 2'-ethylphenyl moiety of ganstigmine to *TcAChE*. H bonds are represented as dashed lines. Note that Glu199 stabilizes the position and orientation of the imidazole ring of His440.

strong hydrogen bond may provide an explanation for the inhibitory activity of ganstigmine and some of its derivatives. Indeed, the catalytic triad is not disrupted as a result of substantial change in the position of the imidazole ring of the histidine residue, as observed in the *TcAChE*–rivastigmine conjugate.<sup>38</sup> Instead, the deactivation results from the presence of a hydrogen bond between  $N^{\epsilon 2}$  and the covalently bound carbamic moiety of the inhibitor, which locks the catalytic histidine His440. Thus  $N^{\epsilon 2}$  is no longer available to a neighboring water molecule, essential in the deacylation step, which in turn is necessary for the reactivation of the enzyme (Figure 4).

The molecular geometry and conformational parameters of the carbamate moiety in the known 3D crystal structures of carbamoylated *TcAChE*-conjugates have been compared in Table 1.

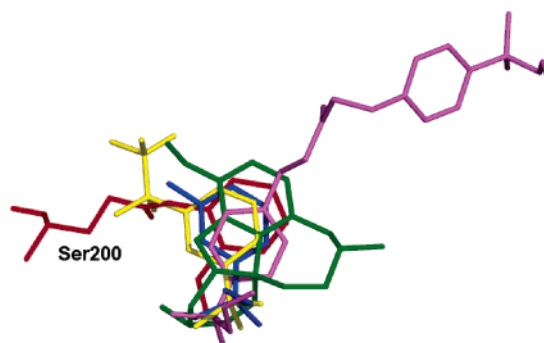
Interestingly, in the rivastigmine–*TcAChE* conjugate<sup>38</sup> a different orientation of the carbamoylated moiety in the active center is observed, as indicated by the  $C^\beta$ - $O'$ - $C$ - $N$  torsion angle of 168.9°, whereas the corresponding values in the MF268–<sup>28</sup> and 3–*TcAChE* conjugates are –126.8° and –115.2°, respec-

**Table 1.** Molecular Geometry of the Carbamate Moiety in Carbamoylated *Torpedo californica* AChE Complexes


	MF268 (pdb ID 1OCE)	rivastigmine (pdb ID 1GQR)	ganstigmine (3)
Compound			
R1	H	methyl	H
R2	<i>cis</i> -2,6-(dimethyl morpholino)octyl	ethyl	2'-ethylphenyl
Bond lengths (°)			
C <sup>α</sup> –C <sup>β</sup>	1.54	1.53	1.54
C <sup>β</sup> –O <sup>γ</sup>	1.43	1.39	1.41
O <sup>γ</sup> –C	1.37	1.44	1.37
C–O	1.22	1.24	1.21
C–N	1.42	1.53	1.34
N–C <sub>R1</sub>	1.47	1.50	1.44
N–C <sub>R2</sub>		1.42	
Bond angles (°)			
C <sup>α</sup> –C <sup>β</sup> –O <sup>γ</sup>	112.2	102.8	113.1
C <sup>β</sup> –O <sup>γ</sup> –C	117.5	112.3	117.5
O <sup>γ</sup> –C–O	120.7	117.8	124.1
O <sup>γ</sup> –C–N	118.8	113.9	108.6
O–C–N	120.5	109.7	127.3
C–N–C <sub>R1</sub>	120.9	123.3	125.1
C–N–C <sub>R2</sub>		116.4	
Torsion angles (°)			
C <sup>α</sup> –C <sup>β</sup> –O <sup>γ</sup> –C	–143.4	–132.1	–137.0
C <sup>β</sup> –O <sup>γ</sup> –C–O	53.3	38.4	63.3
C <sup>β</sup> –O <sup>γ</sup> –C–N	–126.8	168.9	–115.2
O <sup>γ</sup> –C–N–C <sub>R1</sub>	170.5	–171.7	169.8
O <sup>γ</sup> –C–N–C <sub>R2</sub>		–9.8	
O–C–N–C <sub>R1</sub>	–9.7	–37.4	–8.6
O–C–N–C <sub>R2</sub>		124.5	

tively. Moreover, the molecular geometry of the N atom belonging to the carbamic moiety is trigonal planar in the MF268<sup>28</sup> and **3**–*TcAChE* conjugates, whereas in the rivastigmine–*TcAChE* conjugate,<sup>38</sup> it is significantly pyramidalized.

In the structure of **3** with *TcAChE*, there is a continuous electron density at the 2σ contouring level between Ser200 O<sup>γ</sup> and the C of the carbamic moiety of ganstigmine. The distance of 1.37 Å between the atoms involved confirms the presence of a covalent bond. The carbamic moiety is further stabilized by hydrogen bonds between the carbonyl oxygen and the NH of Gly118 and Gly119 residues, forming the oxyanion hole, distances being 2.59 and 2.54 Å, respectively. The carbonyl oxygen also interacts with the NH of Ala201 (2.96 Å). As previously observed in the structures of organophosphorus acid anhydride nerve agents in complex with *TcAChE*, this remarkable array of noncovalent forces provides a structural barrier to enzyme reactivation.<sup>45</sup> The tripartite array, Glu327–His440–Glu199, may be considered a structural device for productively orienting the imidazole ring according to the steric and the electrostatic features of the ligand bound to Ser200. The *TcAChE* Glu199Gln mutation was found to reduce the  $k_{cat}/K_m$  value for hydrolysis of optimal ester substrates by 50–100 fold, suggesting that Glu199 provides a specific stabilization of the transition state in the acylation stage of catalysis.<sup>46</sup> Moreover, a cryptic catalytic mechanism, which relies upon Glu199 during the hydrolysis of relatively slow-reacting carboxyl ester substrates, has been proposed.<sup>47</sup> Remarkably, the comparison of the structures of recombinant native and Glu202Gln mutant human AChE showed that the removal of the charged group

**Figure 5.** Overlay of the 2'-ethylphenyl moiety of ganstigmine (red) covalently bound to *TcAChE* catalytic residue Ser200 and selected *TcAChE* conjugate crystal structures. Stick representation of the bound conformation of galanthamine<sup>49,50</sup> (green), edrophonium<sup>51,52</sup> (blue), the transition state analogue  $\mu$ -(*N,N',N''*-trimethylammonium)trifluoroacetophenone<sup>53</sup> (yellow), and Bw284C51<sup>54</sup> (magenta) inhibitors are shown. For clarity, the protein residues have been omitted.

from the protein core and its substitution by a neutral isosteric moiety does not disrupt the functional architecture of the active center.<sup>48</sup>

There are no additional contacts between the (2'-ethylphenyl) carbamic moiety and neighboring protein residues or water molecules. Nevertheless, the 2'-ethylphenyl moiety shows a binding orientation in the active site of the enzyme that largely overlaps with those observed for the phenyl ring functionality in the crystal structures of *TcAChE* complexed with galanthamine,<sup>49,50</sup> edrophonium,<sup>51,52</sup> the transition state analogue  $\mu$ -(*N,N',N''*-trimethylammonium)trifluoroacetophenone,<sup>53</sup> and Bw284C51.<sup>54</sup> In particular, the aromatic rings are oriented almost parallel to each other with angles of 10.6°, 10.6°, 15.6°, and 7.8° and displaced by average distances of 0.82 Å, 0.84 Å, 1.09 Å, and 1.31 Å, respectively. Clearly, these reversible and nonreversible inhibitors share a common binding area at the bottom of the active-site gorge (Figure 5).

The precipitant solution used for crystallizing the *TcAChE*–ganstigmine conjugate contains poly(ethylene glycol) PEG-200. In the present structure, a short pentameric fragment of PEG unexpectedly occupies part of the active-site gorge. The crystal structure determination of a complex of *TcAChE* with an uncharged inhibitor, PEG-SH-350 (containing mainly heptameric poly(ethylene glycol) with a terminal thiol group), has recently been reported.<sup>55</sup> The overlay of this inhibitor with the PEG molecule in the present structure showed that they are similarly oriented. Furthermore, the side chains orientations of all aromatic residues, within the active-site gorge, including the conformational flexible side chain of the swinging gate residue Phe330, are unchanged. Interestingly, the extended octyl alkyl chain of the MF268 inhibitor adopts a similar conformation along the active-site gorge.<sup>28</sup>

The active-site gorge of the native enzyme is filled with over 20 water molecules, which have poor hydrogen-bond coordination with an average of 2.9 polar contacts per water molecule.<sup>56</sup> The acyl pocket may provide another barrier to reactivation. Indeed, a dry hydrophobic patch formed by Phe288, Phe290, Trp233, and C<sup>α</sup> of Gly119 surrounds the 2'-ethylphenyl moiety of ganstigmine. Different inhibitors displace different water molecules. Namely, in the crystal structures of the *TcAChE*–MF268,<sup>28</sup> *TcAChE*–rivastigmine,<sup>38</sup> and *TcAChE*–ganstigmine conjugates, 12, 7, and 8 water molecules, respectively, which are observed in the native enzyme and are positioned in the lower part of the active-site gorge, are displaced.<sup>56</sup> No novel structured water molecules are observed.



**Table 2.** *Torpedo californica* AChE Inhibition in Vitro

compd <sup>a</sup>	IC <sub>50</sub> values (μM)	95% confidence limits (μM)
rivastigmine	187.2	(137.5–225.0)
geneserine	1.74	(1.46–2.08)
<b>1</b>	4.74	(4.13–5.46)
<b>2</b>	4.04	(3.83–4.27)
<b>3</b>	5.12	(4.38–7.76)
<b>4</b>	8.38	(7.64–9.20)
<b>5</b>	8.44	(7.55–9.19)
<b>6</b>	5.13	(3.75–8.84)
<b>7</b>	9.80	(1.97–15.63)
<b>8</b>	7.61	(6.84–9.29)
<b>9</b>	186.0	(161.8–213.7)
<b>10</b>	8.58	(7.83–9.41)

<sup>a</sup> All compounds refer to the HCl salt form with the exception of rivastigmine (tartrate).

**Table 3.** CD-1 Mice Brain AChE Inhibition ex Vivo<sup>a</sup>

compd	dose (mg/kg p.o.)	peak of inhibition (%)	T <sub>pk</sub> (h)	duration (h)
rivastigmine	1.5	73	0.5	4
geneserine	1.3	37	0.5	4
<b>1</b>	11	50	0.5	6
<b>2</b>	3.4	45	0.5	6
<b>3</b>	3.4	28	4	6
<b>4</b>	3.4	30	4	6
<b>5</b>	3.4	28	6	6
<b>6</b>	11	57	1	6
<b>7<sup>b</sup></b>	30	41	0.5	6
<b>8<sup>b</sup></b>	50	26	0.5	6
<b>9<sup>b</sup></b>	11	13	6	6
<b>10</b>	11	54	2	6

<sup>a</sup> The results are reported as peak % inhibition, time of peak, and duration of AChE inhibition expressed as observation time points that were significantly different from those of untreated controls ( $p \leq 0.05$ ). <sup>b</sup> The activity of these compounds was tested only at 0.5 and 6 h after treatment.

**Structure–Activity Relationships of Geneserine Analogues.** The analysis of the *TcAChE*–**3** complex allows the rationalization of the observed differences in inhibitory activity of several aryl GEN derivatives evaluated in vitro on purified *TcAChE* (Table 2) as well as ex vivo on CD1 male mice brain AChE after oral administration (Table 3).

Specifically, in vitro data show that chemical modifications of the phenyl ring at any position other than 2 cause a partial loss of inhibitory activity. A comparison of compounds bearing the same substituent indicates a constant decrease in activity when moving along the aromatic ring from position 2 (compound **2**) to position 4 (compound **8**). This is found both in the case of a methyl substituent (compounds **2**, **6**, **8**) as well as an ethyl group (compounds **3** and **7**). Indeed, even small substituents would probably require a conformational rearrangement for the ligand to be accommodated at the base of the catalytic gorge of the enzyme. Bulky substituents, however, decrease activity even if they are present at position 2 (compounds **4** and **5**). Studies ex vivo further extend the observations of studies in vitro. Indeed, compounds bearing a substitution in position 2 of the phenyl ring are the most potent inhibitors of brain AChE. Moreover, compounds **3**–**5** at 3.4 mg/kg effectively inhibit brain AChE up to 6 h after administration, with a peak effect at 4–6 h, indicating that these compounds are long-lasting inhibitors of brain AChE. However, it should be taken into account that factors other than the affinity for the enzyme, such as absorption, biotransformation, and blood–brain barrier penetration, may have influenced the outcome of the ex vivo studies.

An analysis of the interacting pattern of the 2'-ethylphenyl carbamic moiety and the relative distances with the surrounding protein residues, located at the bottom of the active-site gorge, explains this behavior.

The C-3 of the phenyl ring is not close to any protein residue; however it is 3.52 Å apart from the water molecule W103 (W603 in the native structure, pdb accession code: 2ACE). The C-4 of the phenyl ring of the 2'-ethylphenyl moiety is 3.16 and 4.37 Å apart from the OH group of Tyr121 and the carbonyl group of Gly118, respectively. This observation may explain why compound **8**, methylated at position 4, shows ca. 2-fold loss of inhibitory activity in vitro with respect to compound **2**, methylated at position 2. The C-5 of the phenyl ring is 3.15 Å apart from the OH group of Tyr121, and it is in close contact with both C<sup>ε</sup> and C<sup>ε</sup>1 of Phe290 (4.30 Å) and with C<sup>ε</sup>2 of Phe331 (4.31 Å). Accordingly, the activity of **10**, methylated at positions 3 and 5, is reduced approximately 2-fold relative to that of **6**, which is only methylated at C-3. The C-6 of the phenyl ring is 3.86 Å apart from the C<sup>α</sup> of Gly119 and the C<sup>ε</sup> of Phe290 and 3.94 Å apart from the C<sup>ε</sup> of Phe331. Thus, the C-6 position of the aryl moiety seems to be the one most sensitive to further substitutions in comparison to all other positions, as indicated by compound **9**, which shows a complete loss of activity while differing from compound **2** by being methylated also at C-6. This latter additional substitution by disrupting the oxyanion hole prevents the formation of a stable enzyme–carbamate adduct. Overall, in vitro studies suggest ganstigmine (**3**) to be a mechanism-based irreversible inhibitor of AChE, whereas the stability of the enzyme adduct, pointed out by the present crystal structure determination and by enzyme reactivation experiments (Professor K. Tipton, personal communication), explains the long-lasting anti-AChE effect observed both in pharmacological and in clinical studies.<sup>17,25</sup>

**Significance.** AD is the most common form of neurodegenerative loss of normal brain function, including thought, memory, and language. Besides the neuropathologic hallmarks of the disease, namely, neurofibrillary tangles and neuritic plaques, AD is characterized neurochemically by a consistent deficit in cholinergic neurotransmission, particularly affecting cholinergic neurons in the basal forebrain. The evidence stems from data of enzymes involved in the synthesis, cholinacetyltransferase, or the degradation, acetylcholinesterase, of acetylcholine. Alterations in the overall observation of a cholinergic deficit in AD patients led to the cholinergic boosting strategies in the treatment of AD. Following tacrine, the first AChE inhibitor specifically approved for the treatment of AD, several AChE inhibitors, such as donepezil, rivastigmine, galanthamine, and metrifonate, were made available for the symptomatic treatment of patients with mid-to-moderate AD. Recently, the clinical profile of a novel carbamate-based, orally active AChE inhibitor, ganstigmine, was evaluated, and this compound showed potential for the treatment of AD.<sup>25</sup> It is a selective inhibitor, more potent against AChE than BuChE (115-fold higher selectivity) and also more selective (10-fold) for the inhibition of central rather than peripheral AChE.<sup>21</sup> It shows significant neurochemical effects in vivo in rats including attenuation of scopolamine-induced amnesia.<sup>26</sup> Long-term treatment in AD patients suggests a potential protective effect because ganstigmine stimulates the release of a soluble non-amyloidogenic form of the amyloid precursor protein in human neuroblastoma cells<sup>23</sup> and protects neurons from toxicity induced by the β-amyloid (25–35) peptide.<sup>24</sup> The crystal structure of the *TcAChE*–ganstigmine conjugate permits a detailed structure-based analysis in vitro on *TcAChE* and ex vivo on CD1 mice

brain, anti-AChE activity by ganstigmine, and by new generine derivatives. Moreover, the structure offers an explanation for the inactivation of the AChE catalytic triad. For the first time, a strong hydrogen bond has been observed between H440 and the carbamoyl moiety of the inhibitor that may account for the long duration of the inhibition of ganstigmine in vivo. The 3D structure also provides a structural framework for the design of novel mechanism-based anti-cholinesterase compounds with improved binding affinity and drug-like properties.

## Experimental Section

**Crystallization and Data collection.** Ganstigmine (**3**) was synthesized at Chiesi Farmaceutici S.p.A and was used for crystallization without further purification. *TcAChE* was extracted, purified, and crystallized as previously described.<sup>57</sup> Crystals, obtained by the hanging drop vapor diffusion method, grew in 2–3 weeks up to a size of  $150 \times 150 \times 200 \mu\text{m}^3$ . The crystals of *TcAChE* in complex with ganstigmine were obtained by soaking the native AChE crystals in 10 mM **3**, 42% PEG200, 100 mM MES at pH 6.0 for 24 h at 4 °C.

X-ray diffraction data to 2.4 Å resolution were collected at the XRD-1 beam line of the Italian synchrotron facility *ELETTRA*, Trieste, Italy ( $\lambda = 1.00 \text{ \AA}$ ). A Mar345 imaging plate system (X-ray Research, Hamburg, Germany) and focusing optics were employed for the measurements. Eighty-five images were collected, and a 1.2° oscillation range was used for all images. The crystals were flash-cooled in a nitrogen stream at 120 K, using an Oxford Cryosystem cooling device (Oxford, U.K.). Oscillation data were indexed, integrated, scaled, and reduced using DENZO, SCALEPACK,<sup>58</sup> and the CCP4<sup>59</sup> package. The degree of linear polarization was assumed to be 0.95, and the mosaic spread of the crystal was estimated to be 0.73°. Crystals belong to the trigonal system with unit cell  $a = b = 111.74 \text{ \AA}$  and  $c = 136.82 \text{ \AA}$  and space group  $P3_121$ . The unit cell volume is consistent with one *TcAChE* molecule in the crystal asymmetric unit with a Matthews's coefficient of  $4.0 \text{ \AA}^3/\text{Da}$ , corresponding to 69.2% solvent content.<sup>60</sup>

**Structure Determination and Refinement.** We determined the crystal structure of *TcAChE* by Patterson search methods using the native *TcAChE* structure,<sup>61</sup> pdb ID accession code 2ACE<sup>29,30</sup> as a search model, after removing all solvent molecules. Crystallographic refinement of the *TcAChE*–**3** complex was performed with CNS version 1.0.<sup>62</sup> All data between 28.0 and 2.40 Å were included with no-sigma cutoff. A bulk solvent correction and anisotropic scaling were applied. The Fourier maps were computed with SIGMA-A weighted  $(2|F_o| - |F_c|, \phi_c)$  and  $(|F_o| - |F_c|, \phi_c)$  coefficients<sup>63</sup> after initial refinement of the native protein by simulated annealing (at a maximum temperature of 3000 K), followed by maximum likelihood positional and isotropic temperature factor refinements. A prominent difference electron density feature in the catalytic gorge clearly indicated the presence of the 2'-ethylphenyl moiety of **3**, covalently bound to the O<sup>γ</sup> of Ser200. Map interpretation was performed using the program O.<sup>64</sup> The maps also clearly revealed and allowed the tracing of the loop connecting residues 481 to 493, which was absent in the 2ACE-searching model. A few side chains were manually adjusted, and PEG, MES, and carbohydrates ( $\beta$ -D-N-acetyl glucosamine linked at Asn494 and Asn498) molecules were built-in by inspecting electron density maps. Water molecules, peaks at a contour level of  $2.5\sigma$  on the  $(|F_o| - |F_c|, \phi_c)$  map, were automatically added to the atomic model and retained if they met stereochemical requirements and their B factor was less than  $70 \text{ \AA}^2$  after refinement. The CNS topology and parameter files for the 2'-ethylphenyl moiety were generated with the program PRODRG<sup>65</sup> using the crystal structure of **3** (Pelizzi G., and Bacchi, A., personal communication). The crystal parameters, data collection, and refinement statistics are summarized in Table 4. Structure alignment and root-mean-square deviation (RMSD) calculations were done using the program LSQMAN.<sup>70</sup> Figures were created using PyMOL.<sup>71</sup>

**Pharmacology: Quantitation of Anticholinesterase Activity. *TcAChE* Activity in Vitro.** The in vitro action of generine,

**Table 4.** Summary of Crystallographic Data of the *Torpedo californica* AChE–Ganstigmine Complex

Data Collection	
X-ray source	XRD-1 ELETTRA, Trieste (Italy)
wavelength (Å)	1.00
detector	Mar345
space group	$P3_121$
unit cell parameters	
$a, b$ (Å)	111.74
$c$ (Å)	136.82
mosaicity (°)	0.73
resolution range (Å)	27.95–2.40 (2.44 – 2.40) <sup>a</sup>
number of measurements	517559
number of observed reflections ( $I \geq 0$ )	228580 (11735)
number of unique reflections ( $I \geq 0$ )	37817 (2303)
completeness (%)	96.4 (97.4)
multiplicity	6.0 (5.1)
$\langle I/\sigma(I) \rangle$	8.6 (1.9)
$R_{\text{sym}}^b$	0.063 (0.470)
$R_{\text{measured}}^c$	
Refinement Statistics	
resolution range (Å)	27.95–2.40
number of reflections ( $F_o \geq 0$ )	37576
$R^d$	0.190
$R_{\text{free}}^e$	0.236
number of atoms	
nonhydrogen protein	4245
solvent molecules	274
nonhydrogen inhibitor	11
nonhydrogen carbohydrate	28
nonhydrogen PEG	16
nonhydrogen buffer	24
RMSD bond lengths/bond angles (Å, deg) <sup>f</sup>	0.010/1.597
Ramachandran plot favored/allowed/generously allowed (%) <sup>g</sup>	90.7/8.6/0.7
Average Temperature Factors (Å <sup>2</sup> )	
protein	44.8
water	48.8
inhibitor	50.8
carbohydrates	74.2
PEG	82.1
MES buffer	94.1
RMSD $\Delta B$ (Å <sup>2</sup> ) <sup>h</sup>	4.23

<sup>a</sup> Numbers in parentheses refer to the highest resolution shell. <sup>b</sup>  $R_{\text{sym}} = \sum_h \sum_i |I_{hi} - \langle I_h \rangle| / \sum_h \sum_i I_{hi}$ , where  $I_h$  is the  $i$ th measurement of reflection  $h$ , and  $\langle I_h \rangle$  is the average over symmetry related observations of unique reflection  $h$ . The summations include all observed reflections. <sup>c</sup>  $R_{\text{meas}}$  is the multiplicity weighted  $R_{\text{sym}}$ . <sup>d</sup>  $R = \sum_h |F_o| - |F_c| / \sum_h |F_o|$ , where  $|F_o|$  and  $|F_c|$  are the observed and calculated structure factor amplitudes, respectively, for reflection  $h$ . The summation is extended over all unique reflections to the specified resolution. <sup>e</sup>  $R_{\text{free}}$  is the  $R$  factor calculated using 3762 randomly chosen reflections (10%) set aside from all stages of refinement. <sup>f</sup> Stereochemical criteria are those of Engh and Huber.<sup>67</sup> <sup>g</sup> Residue Ser200 is in the generously allowed region.<sup>68</sup> <sup>h</sup> RMSD  $\Delta B$  is the RMS deviation of the  $B$  factor of bonded atoms (all atoms).<sup>69</sup>

rivastigmine, and compounds **1–10** to inhibit the ability of freshly prepared *Torpedo californica*, AChE derived from the electric organ,<sup>57</sup> to enzymatically degrade the specific substrate acetylthiocholine iodide (ATCh) (Sigma-Aldrich S.r.l., Milano, Italy), was quantified using a modified Ellman's method.<sup>72</sup> The principle of this method is based on the production of thiocholine from acetylthiocholine iodide by AChE. Thiocholine reacts with the reagent 5,5'-dithiobis-2-nitrobenzoic acid (DTNB), the so-called Ellman's reagent, an mercaptothiocholine-2-nitrobenzoate and

2-nitro-5-mercaptobenzoic acid to produce a yellow color. The rate of hydrolysis by AChE has been monitored spectrophotometrically at  $\lambda = 415$  nm. The cholinesterase inhibition assay has been adapted to a 96-well micro plate format, allowing for three compounds to be assayed at the same time, in triplicate and in a range of eight different concentrations that differ by approximately a half-log factor.

Appropriate amounts (0.00125 U) of AChE (specific activity 1900 U/mg) at the optimal working pH 8.0 in 0.1 M  $\text{Na}_3\text{PO}_4$  were utilized. Compounds were dissolved in DMSO and diluted in 0.1 M  $\text{Na}_3\text{PO}_4$  buffer (pH 8.0). The compounds were preincubated with AChE (60 min, r.t.) and then were incubated (r.t.) with DTNB and ATCH. Production of a yellow thionitrobenzoate anion was measured for 6 min, at a time interval of 2 min (4 measurements).

To correct for nonspecific substrate hydrolysis, aliquots were co-incubated under conditions of an absence of enzyme, and the associated alteration in absorbance was subtracted from that observed in samples measured in the same plate.

The enzyme activity at each concentration of test compound was expressed as a percent of the activity in the absence of compound. For each compound, the  $\text{IC}_{50}$  value was calculated using Graph Pad software and plotting the log [concentration] versus effect (% of AChE activity) and assuming a sigmoidal curve model.

**Mice Brain AChE Activity ex Vivo.** Groups of 6–9 male CD-1 mice were dosed orally with test compounds and sacrificed at different intervals of time (up to 6 h after treatment). Mice were fasted overnight ( $\approx 17$  h) before oral dosing. The activity of the compounds tested was evaluated at doses supposed to be equiactive, that is, doses equal to 1/7 of the  $\text{LD}_{50}$  values determined in preliminary experiments. Residual AChE activity was determined according to the method of Ellman.<sup>72</sup> Briefly, brains were homogenized in 0.5 mL of phosphate buffer (pH 8.0) added with 1% Triton 100. The homogenate was centrifuged at 19 943g for 15 min at 4 °C. The resultant supernatant was used for AChE activity determination.

**Acknowledgment.** We thank Professor G. Pelizzi and Professor A. Bacchi (Dip. di Chimica Generale ed Inorganica, Chimica Analitica, Chimica Fisica, Università di Parma, Parma, Italy) for kindly providing the atomic coordinates of ganstigmine. We gratefully acknowledge Professor K. Tipton (Department of Biochemistry, Trinity College, Dublin, Ireland) for the in vitro enzyme reactivation kinetic data, the staff of the XRD1 beam line at the ELETTRA synchrotron facility (Trieste, Italy) for their support, and Dr. Emanuele Perola (Vertex Pharmaceuticals Inc., Cambridge, MA) for helpful discussions and the critical reading of this manuscript.

## References

- Barnes, L. L.; Wilson, R. S.; Schneider, J. A.; Bienias, J. L.; Evans, D. A.; Bennett, D. A. Gender, cognitive decline, and risk of AD in older persons. *Neurology* **2003**, *60*, 1777–1781.
- Citron, M. Strategies for disease modification in Alzheimer's disease. *Nat. Rev. Neurosci.* **2004**, *5*, 677–685.
- Terry, A. V.; Buccafusco, J. J. The cholinergic hypothesis of age and Alzheimer's disease-related cognitive deficits: recent challenges and their implications for novel drug development. *J. Pharmacol. Exp. Ther.* **2003**, *306*, 821–827.
- Giacobini, E. Cholinergic function and Alzheimer's disease. *Int. J. Geriatr. Psychiatr.* **2003**, *18*, S1–S5.
- Silman, I.; Sussman J. L. Acetylcholinesterase: 'classical' and 'non-classical' functions and pharmacology. *Curr. Opin. Pharmacol.* **2005**, *5*, 293–302.
- Soreq, H.; Seidman S. Acetylcholinesterase-new roles for an old actor. *Nat. Rev. Neurosci.* **2001**, *2*, 294–302.
- Meshorer, E.; Soreq, H. Virtues and woes of AChE alternative splicing in stress-related neuropathologies. *Trends Neurosci.* **2006**, *29*, 216–224.
- Brufani, M.; Marta, M.; Pomponi, M. Anticholinesterase activity of a new carbamate, heptylphosphostigmine, in view of its use in patients with Alzheimer-type dementia. *Eur. J. Biochem.* **1986**, *157*, 115–120.
- Greig, N. H.; Pei, X. F.; Soncrant, T. T.; Ingram, D. H.; Brossi, A. Phenserine and ring C hetero-analogues: drug candidates for the treatment of Alzheimer's disease. *Med. Res. Rev.* **1995**, *15*, 3–31.
- Zhu, X. D.; Cuadra, G.; Brufani, M.; Maggi, T.; Pagella, P. G.; Williams, E.; Giacobini, E. Effects of MF-268, a new cholinesterase inhibitor, on acetylcholine and biogenic amines in rat cortex. *J. Neurosci. Res.* **1996**, *43*, 120–126.
- Perola, E.; Cellai, L.; Lamba, D.; Filocamo, L.; Brufani, M. Long chain analogs of phisosti-gmine as potential drugs for Alzheimer's disease: new insights into the mechanism of action in the inhibition of acetylcholinesterase. *Biochim. Biophys. Acta* **1997**, *1342*, 41–50.
- Braida, D.; Paladini, E.; Griffini, P.; Lamperti, M.; Colibretti, L.; Sala, M. Long-lasting anti-amnesic effect of a novel anticholinesterase inhibitor (MF268). *Pharmacol., Biochem. Behav.* **1998**, *59*, 897–901.
- Liston, D. R.; Nielsen, J. A.; Villalobos, A.; Chapin, D.; Jones, S. B.; Hubbard, S. T.; Shalaby, I. A.; Ramirez, A.; Nason, D.; White, W. F. Pharmacology of selective acetylcholinesterase inhibitors: implications for use in Alzheimer's disease. *Eur. J. Pharmacol.* **2004**, *486*, 9–17.
- Yu, Q.-S.; Yeh, H. J. C.; Brossi, A.; Flippen-Anderson, J. L. Geneserine and geneseroline revisited: acid-base-catalyzed equilibria of hexahydropyrrolo-[2,3-b]-indole N-oxides with hexahydro-1,2-oxazino-[5,6-b]-indoles. *J. Nat. Prod.* **1989**, *52*, 331–336.
- Bacchi A.; Pelizzi, G.; Redenti, E.; Delcanale, M.; Amari, G.; Ventura, P. Geneserine hydrochloride. *Acta Crystallogr., Sect. C* **1994**, *50*, 1126–1130.
- Redenti, E.; Delcanale, M.; Amari, G.; Ventura, P.; Bacchi, A.; Pelizzi, G. Solution- and solid-state structures of the (–)-n-heptyl-carbamate of geneseroline and its hydrochloride salt. *J. Pharm. Sci.* **1995**, *84*, 1126–1133.
- Pietra, C.; Villetti, G.; Bolzoni, P. T.; Delcanale, M.; Amari, G.; Caruso, P.; Civelli, M. Cholinesterase Inhibitory Activity of New Geneserine Derivatives. In *Alzheimer Disease and Related Disorders*; Iqbal, K., Swaab, D. F., Winbald, B., Wisniewski, H. M., Eds.; John Wiley & Sons: New York, 1999; pp 689–696.
- Trabace, L.; Cassano, T.; Steardo, L.; Pietra, C.; Villetti, G.; Kendrick, K. M.; Cuomo, V. Biochemical and neurobehavioral profile of CHF2819, a novel, orally active acetylcholinesterase inhibitor for Alzheimer's disease. *J. Pharmacol. Exp. Ther.* **2000**, *294*, 187–194.
- Catinella, S.; Pelizzi, N.; Puccini, P.; Marchetti, S.; Zanol, M.; Acerbi, D.; Ventura, P. Phase I metabolism of ganstigmine. Rat, dog, monkey and human liver microsomal extracts investigated by liquid chromatography electrospray tandem mass spectrometry. *J. Mass Spectrom.* **2001**, *36*, 1287–1293.
- Trabace, L.; Cassano, T.; Cagiano, R.; Tattoli, M.; Pietra, C.; Steardo, L.; Kendrick, K. M.; Cuomo, V. Effects of ENA713 and CHF2819, two anti-Alzheimer's disease drugs, on rat amino acid levels. *Brain Res.* **2001**, *910*, 182–186.
- Trabace, L.; Cassano, T.; Loverre, A.; Steardo, L.; Cuomo, V. CHF2819: pharmacological profile of a novel acetylcholinesterase inhibitor. *CNS Drug Rev.* **2002**, *8*, 53–69.
- Cassano, T.; Carratù, M. R.; Cosuccia, A.; Di Giovanni, V.; Steardo, L.; Cuomo, V.; Trabace, L. Preclinical progress with CHF2819, a novel orally active acetylcholinesterase inhibitor. *Drug Dev. Res.* **2002**, *56*, 354–368.
- Mazzucchelli, M.; Porrello, E.; Villetti, G.; Pietra, C.; Govoni, S.; Racchi, M. Characterization of the effect of ganstigmine (CHF2819) on amyloid precursor protein metabolism in SH-SY5Y neuroblastoma cells. *J. Neural Transm.* **2003**, *110*, 935–947.
- Windisch, M.; Hutter-Paier, B.; Jerkovic, L.; Imbimbo, B.; Villetti, G. The protective effect of ganstigmine against amyloid beta 25–35 neurotoxicity on chicken cortical neurons is independent from the cholinesterase inhibition. *Neurosci. Lett.* **2003**, *341*, 181–184.
- Jhee, S. S.; Fabbri, L.; Piccinno, A.; Monici, P.; Moran, S.; Zarotsky, V.; Tan, E. Y.; Frackiewicz, E. J.; Shiovtz, T. First clinical evaluation of ganstigmine in patients with probable Alzheimer's disease. *Clin. Neuropharmacol.* **2003**, *26*, 164–169.
- Capsoni, S.; Giannotta, S.; Stebel, M.; Garcia, A. A.; De Rosa, R.; Villetti, G.; Imbimbo, B. P.; Pietra, C.; Cattaneo, A. Ganstigmine and donepezil improve neurodegeneration in AD11 antinerve growth factor transgenic mice. *Am. J. Alzheimer's Dis. Other Dement.* **2004**, *19*, 153–160.
- Yu, Q. S.; Zhu, X.; Holloway, H. W.; Whittaker, N. F.; Brossi, A.; Greig, N. H. Anticholinesterase activity of compounds related to geneserine tautomers. N-oxides and 1,2-oxazines. *J. Med. Chem.* **2002**, *45*, 3684–3691.
- Bartolucci, C.; Perola, E.; Cellai, L.; Brufani, M.; Lamba, D. "Back door" opening implied by the crystal structure of a carbamoylated acetylcholinesterase. *Biochemistry* **1979**, *18*, 5714–5719.



- (29) Raves, M. L.; Harel, M.; Pang, Y.-P.; Silman, I.; Kozikowski, A. P.; Sussman, J. L. 3D structure of acetylcholinesterase complexed with the nootropic alkaloid, (-)-huperzine A. *Nat. Struct. Biol.* **1997**, *4*, 57–63.
- (30) Berman, H. M.; Westbrook, J.; Feng, Z.; Gilliland, G.; Bhat, T. N.; Weissig, H.; Shindyalov, I. N.; Bourne, P. E. The protein data bank. *Nucleic Acids Res.* **2000**, *28*, 235–242.
- (31) Gilson, M. K.; Straatsma, T. P.; McCammon, J. A.; Ripoll, D. R.; Faerman, C. H.; Axelsen, P. H.; Silman, I.; Sussman, J. L. Open “back door” in a molecular dynamics simulation of acetylcholinesterase. *Science* **1994**, *263*, 1276–1278.
- (32) Kronman, C.; Ordentlich, A.; Barak, D.; Velan, B.; Shafferman, A. The “back door” hypothesis for product clearance in acetylcholinesterase challenged by site-directed mutagenesis. *J. Biol. Chem.* **1994**, *269*, 27819–27822.
- (33) Faerman, C.; Ripoll, D.; Bon, S.; Le Feuvre, Y.; Morel, N.; Massoulié, J.; Sussman, J. L.; Silman, I. Site-directed mutants designed to test back-door hypotheses of acetylcholinesterase function. *FEBS Lett.* **1996**, *386*, 65–71.
- (34) Botti, S. A.; Felder, C. E.; Lifson, S.; Sussman, J. L.; Silman, I. A modular treatment of molecular traffic through the active site of cholinesterase. *Biophys. J.* **1999**, *77*, 2430–2450.
- (35) Alisaraie, L.; Fels, G. Molecular docking study on the “back door” hypothesis for product clearance in acetylcholinesterase. *J. Mol. Model.* **2006**, *12*, 348–354.
- (36) Greenblatt, H. M.; Guillou, C.; Guénard, D.; Argaman, A.; Botti, S.; Badet, B.; Thal, C.; Silman, I.; Sussman, J. L. The complex of a bivalent derivative of galanthamine with *Torpedo* acetylcholinesterase displays drastic deformation of the active-site gorge: implications for structure-based drug design. *J. Am. Chem. Soc.* **2004**, *126*, 15405–15411.
- (37) Colletier, J.-P.; Fournier, D.; Greenblatt, H. M.; Stojan, J.; Sussman, J. L.; Zaccai, G.; Silman, I.; Weik, M. Structural insights into substrate traffic and inhibition in acetylcholinesterase. *EMBO J.* **2006**, *25*, 2746–2756.
- (38) Bar-On, P.; Millard, C. B.; Harel, M.; Duir, H.; Enz, A.; Sussman, J. L.; Silman, I. Kinetic and structural studies on the interaction of the cholinesterase with the anti-Alzheimer drug rivastigmine. *Biochemistry* **2002**, *41*, 3555–3564.
- (39) Millard, C. B.; Koellner, G.; Ordentlich, A.; Shafferman, A.; Silman, I.; and Sussman, J. L. Reaction products of acetylcholinesterase and VX reveal a mobile histidine in the catalytic triad. *J. Am. Chem. Soc.* **1999**, *121*, 9883–9884.
- (40) Massiah, M. A.; Viragh, C.; Reddy, P. M.; Kovach, I. M.; Johnson, J.; Rosenberry, T. L.; Midvan, A. S. Short, strong hydrogen bonds at the active site of human acetylcholinesterase: proton NMR studies. *Biochemistry* **2001**, *40*, 5682–5690.
- (41) Barak, D.; Kaplan, D.; Ordentlich, A.; Ariel, N.; Velan, B.; Shafferman, A. The aromatic “trapping” of the catalytic histidine is essential for efficient catalysis in acetylcholinesterase. *Biochemistry* **2002**, *41*, 8245–8252.
- (42) Shafferman, A.; Barak, D.; Kaplan, D.; Ordentlich, A.; Kronman, C.; Velan, B. Functional requirements for the optimal catalytic configuration of the AChE active center. *Chem. Biol. Interact.* **2005**, *157–158*, 123–131.
- (43) Barak, D.; Ordentlich, A.; Kaplan, D.; Kronman, C.; Velan, B.; Shafferman, A. Lessons from functional analysis of AChE covalent and non covalent inhibitors for design of AD therapeutic agents. *Chem. Biol. Interact.* **2005**, *157–158*, 219–226.
- (44) Ekström, F.; Akfur, C.; Tunemalm, A.-K.; Lundberg, S. Structural changes of phenylalanine 338 and histidine 447 revealed by the crystal structures of tabun-inhibited murine acetylcholinesterase. *Biochemistry* **2006**, *45*, 74–81.
- (45) Millard, C. B.; Kryger, G.; Ordentlich, A.; Greenblatt, H. M.; Harel, M.; Raves, M. L.; Segall, Y.; Barak, D.; Shafferman, A.; Silman, I.; Sussman, J. L. Crystal structures of aged phosphonylated acetylcholinesterase: nerve agent reaction products at the atomic level. *Biochemistry* **1999**, *38*, 7032–7039.
- (46) Wlodek, S. T.; Antosiewicz, J.; Briggs, J. M. On the mechanism of acetylcholinesterase action: the electrostatically induced acceleration of the catalytic acylation step. *J. Am. Chem. Soc.* **1997**, *119*, 8159–8165.
- (47) Selwood, T.; Feaster, S. R.; States, M. J.; Pryor, A. N.; Quinn, D. M. Parallel mechanisms in acetylcholinesterase-catalyzed hydrolysis of choline esters. *J. Am. Chem. Soc.* **1993**, *115*, 10477–10482.
- (48) Kryger, G.; Harel, M.; Giles, K.; Toker, L.; Velan, B.; Lazar, A.; Kronman, C.; Barak, D.; Ariel, N.; Shafferman, A.; Silman, I.; Sussman, J. L. Structures of recombinant native and E202Q mutant human acetylcholinesterase complexed with the snake-venom toxin fasciculin-II. *Acta Crystallogr., Sect. D* **2000**, *56*, 1385–1394.
- (49) Greenblatt, H. M.; Kryger, G.; Lewis, T.; Silman, I.; Sussman, J. L. Structure of acetylcholinesterase complexed with (-)galanthamine at 2.3 Å resolution. *FEBS Lett.* **1999**, *463*, 321–326.
- (50) Bartolucci, C.; Perola, E.; Pilger, C.; Fels, G.; Lamba, D. Three-dimensional structure of a complex of galanthamine (Nivalin) with acetylcholinesterase from *Torpedo californica*: implications for the design of new anti-Alzheimer drugs. *Proteins* **2001**, *42*, 182–191.
- (51) Harel, M.; Schalk, I.; Ehret-Sabatier, L.; Bouet, F.; Goeldner, M.; Hirth, C.; Axelsen, P. H.; Silman, I.; Sussman, J. L. Quaternary ligand binding to aromatic residues in the active-site gorge of acetylcholinesterase. *Proc. Natl. Acad. Sci. U. S. A.* **1993**, *90*, 9031–9035.
- (52) Ravelli, R. B.; Raves, M. L.; Ren, Z.; Bourgeois, D.; Roth, M.; Kroon, J.; Silman, I.; Sussman, J. L. Static Laue diffraction studies on acetylcholinesterase. *Acta Crystallogr., Sect. D* **1998**, *54*, 1359–1366.
- (53) Harel, M.; Quinn, D. M.; Nair, H. K.; Silman, I.; Sussman, J. L. The X-ray structure of a transition state analogue complex reveals the molecular origins of the catalytic power and substrate specificity of acetylcholinesterase. *J. Am. Chem. Soc.* **1996**, *118*, 2340–2346.
- (54) Felder, C. E.; Harel, M.; Silman, I.; Sussman, J. L. Structure of a complex of the potent and specific inhibitor Bw284C51 with *Torpedo californica* acetylcholinesterase. *Acta Crystallogr., Sect. D* **2002**, *D58*, 1765–1761.
- (55) Koellner, G.; Steiner, T.; Millard, C. B.; Silman, I.; Sussman, J. L. A neutral molecule in a cation-binding site: specific binding of a PEG-SH to acetylcholinesterase from *Torpedo californica*. *J. Mol. Biol.* **2002**, *320*, 721–725.
- (56) Koellner, G.; Kryger, G.; Millard, C. B.; Silman, I.; Sussman, J. L.; Steiner, T. Active-site gorge and buried water molecules in crystal structures of acetylcholinesterase from *Torpedo californica*. *J. Mol. Biol.* **2000**, *296*, 713–735.
- (57) Sussman, J. L.; Harel, M.; Frolow, F.; Varon, L.; Toker, L.; Futerman, A. H.; Silman, I. Purification and crystallization of a dimeric form of acetylcholinesterase from *Torpedo californica* subsequent to solubilization with phosphatidylinositol-specific phospholipase C. *J. Mol. Biol.* **1988**, *203*, 821–823.
- (58) Otwinowski, Z.; Minor, W. Processing of X-ray diffraction data collected in oscillation mode. *Methods Enzymol.* **1997**, *276*, 307–326.
- (59) Collaborative computational project, number 4. The CCP4 suite: programs for protein crystallography. *Acta Crystallogr., Sect. D* **1994**, *50*, 760–763.
- (60) Matthews, B. W. Solvent content of protein crystals. *J. Mol. Biol.* **1968**, *33*, 491–497.
- (61) Sussman, J. L.; Harel, M.; Frolow, F.; Oefner, C.; Goldman, A.; Toker, L.; Silman, I. Atomic structure of acetylcholinesterase from *Torpedo californica*: a prototypic acetylcholine-binding protein. *Science* **1991**, *253*, 872–879.
- (62) Brünger, A. T.; Adams, P. D.; Clore, G. M.; DeLano, W. L.; Gros, P.; Grosse-Kunstleve, R. W.; Jiang, J.-S.; Kuszewski, J.; Nigels, M.; Pannu, N. S.; Read, R. J.; Rice, L. M.; Simonson, T.; Warren, G. L. Crystallography & NMR system: a new software for macromolecular structure determination. *Acta Crystallogr., Sect. D* **1998**, *54*, 905–921.
- (63) Read, R. J. Improved Fourier coefficients for maps using phases from partial structures with errors. *Acta Crystallogr., Sect. A* **1986**, *42*, 140–149.
- (64) Jones, T. A.; Zou, J.-Y.; Cowan, S. W.; Kjeldgaard, M. Improved methods for building protein models in electron density maps and the location of errors in these models. *Acta Crystallogr., Sect. A* **1991**, *47*, 110–119.
- (65) Schuettelkopf, A. W.; Van Aalten, D. M. F. PRODRG: a tool for high-throughput crystallography of protein–ligand complexes. *Acta Crystallogr., Sect. D* **2004**, *60*, 1355–1363.
- (66) Diederichs, K.; Karplus, P. A. Improved R-factors for diffraction data analysis in macromolecular crystallography. *Nat. Struct. Biol.* **1997**, *4*, 269–275.
- (67) Engh, R. A.; Huber, R. Accurate bond and angle parameters for X-ray protein structure refinement. *Acta Crystallogr., Sect. A* **1991**, *47*, 392–400.
- (68) Laskowski, R. A.; MacArthur, M. W.; Moss, D. S.; Thornton, J. M. PROCHECK: a program to check the stereochemical quality of protein structures. *J. Appl. Crystallogr.* **1993**, *26*, 283–291.
- (69) Kleywegt, G. J. Validation of protein models from C<sub>α</sub> coordinates alone. *J. Mol. Biol.* **1997**, *273*, 371–376.
- (70) Kleywegt, G. J. Use of non-crystallographic symmetry in protein structure refinement. *Acta Crystallogr., Sect. D* **1996**, *52*, 842–857.
- (71) DeLano, W. L. *The PyMOL Molecular Graphics System*; DeLano Scientific LLC, San Carlos, CA. <http://www.pymol.org>.
- (72) Ellman, G. L.; Courtney, K. D.; Andres, A. V., Jr.; Featherstone, R. M. A new and rapid colorimetric determination of acetylcholinesterase activity. *Biochem. Pharmacol.* **1961**, *7*, 88–95.